Application of R2PSO Algorithm in Crack Detection of Functionally Graded Beams

Mojtaba Eftekhari

Department of Mechanical Engineering, Shahid Bahonar University of Kerman, Iran.

Shima Kamyab and Mahdi Eftekhari

Department of Computer Engineering, Shahid Bahonar University of Kerman, Iran.

Mohammad Hosseini

Department of Mechanical Engineering, Sirjan University of Technology, Sirjan, Iran.

(Received 26 December 2014; accepted 4 October 2016)

A fault diagnosis procedure based on r2PSO algorithm—a newly developed version of particle swarm optimization (PSO)—is presented for detecting crack depth and location in a functionally graded material (FGM) cantilever beam. The governing equation and boundary conditions are obtained by using the extended Hamilton's principle, and the characteristic equation is obtained as a function of position ratio and depth ratio of crack. Identification of the crack is formulated as an optimization problem. The r2PSO algorithm is used to find the optimal solution of the cost function, which is based on the summation of the absolute value of the characteristic equation for three natural frequencies. The position ratio and depth ratio of crack are computed by algorithm, when three natural frequencies of FGM beam are entered to algorithm as inputs. The obtained results confirm the applicability and efficiency of r2PSO to calculate the parameters of crack with high accuracy and suitable convergence rate.

1. INTRODUCTION

The existence of a crack in a structural member would change the dynamic behavior of the structure. Changes in overall dynamic of structure present serious threats to performance of the structures such as structure failure. Therefore, many researchers have proposed the different methods to detect and localize the crack in the structures.[1–7] One of the inhomogeneous composite structures is FGM, which have great applications in aerospace vehicles, nuclear reactors, power generators and automobile structures. A crack has occurred in FGM structures and numerous researchers have investigated the fracture analysis of these materials.[3–7]

The location and size of an open edge crack has been determined in an FGM beam by Yu and Chu.[8] They utilized the p-version finite-element method to estimate the transverse vibration of an FGM beam. The influences of crack size, crack location and material gradients have been studied on the natural frequencies of the FGM beam. Numerical experiments have demonstrated the efficiency of their proposed method.

Wei et al.[9] studied free vibration of cracked FGM beams with axial loading, rotary inertia and shear deformation. The model of the crack was the rotational spring model. The influences of the location and total number of cracks, material properties, axial load, inertia and end supports on the natural frequencies of FGM beams have also been studied. Xiang et al. have developed a combination of wavelet-based element and genetic algorithm to detect the location and depth of the crack in a rotating Euler-Bernoulli and Timoshenko beam.[10] Some numerical and experimental results have indicated the performance of their method.

Vakil Baghmishe et al. have proposed the crack identification of a beam as an optimization problem.[11] The cost function of problem was based on the difference of measured and calculated natural frequencies. The binary and continuous genetic algorithms were used to find the optimal location and depth of crack. In order to validate the modeling and method, the results have been presented by some experimental results. An improved particle swarm optimization was developed to detect the damage of structures.[12] The algorithm was a combination of the particle swarm optimization and the artificial immune system. Results have shown the feasibility and efficiency of that improved algorithm.

Nonlinear vibration of the cracked FGM beams has been studied by Kitipornchai and et al.[13] A direct iterative method has been used to find natural frequencies and mode shapes of beam. The effects of crack location, crack depth, slenderness ratio, material property, and boundary conditions were shown on the nonlinear vibration characteristics of the FGM beam.

Fernando and et al.[14] indicated the crack detection in structural elements by means of a genetic algorithm optimization. The methodology has been applied to beam-like structures and any other arbitrary shaped 3-D element. The input data in algorithm has been obtained with a cantilever damaged beam in physical experiments. Birman and Byrd[15] examined free and forced vibration of damaged FGM beam. They modeled the damage to region with degraded stiffness adjacent to the root of the beam, a single delamination crack and a single crack at

the root cross section of the beam. Aydin[16] investigated free vibration of FGM beams containing any arbitrary number of open edge cracks. Miguel and et al.[17] have presented a hybrid stochastic/deterministic algorithm to detect the parameters of crack in cantilever beam. The results were compared to previous works in the literature and the new method was more accurate than the previous methods such as genetic algorithm (GA), harmony search algorithm (HAS) and PSO algorithm. The estimation of a crack location and depth in a cantilever beam has been performed by a hybrid particle swarm Nelder-Mead algorithm.[18] This algorithm was a modified particle swarm optimization algorithm in which a Nelder-Mead algorithm was utilized to perform the local search. The obtained results were compared with the PSO algorithm, a hybrid GA and Nelder-Mead algorithm, and the neural network method. The speed and accuracy of the proposed algorithm was more efficient than the other algorithms. The location and amount of crack has been determined using the neural network by Sahoo and Maity.[19] The neural network was trained by considering the frequency and strain as input and location and amount of crack as output. Robustness of the results proved the good performance of the neural network. Moradi et al. applied the bee algorithm to detect an open edge crack in a cantilever beam.[20] Results showed that the size and location of crack can be predicted well through this algorithm. Multimodal optimization (MO) techniques are a class of optimization methods attempting to find multiple global and local optima of a function. Therefore, the user can have a better knowledge about the search space and when needed, the current solution may be replaced by another optimal one. MO methods, due to their high exploration power, are effective even when the aim is to find a single global optimum. Niching is an important technique for multimodal optimization that usually is incorporated in to a standard Evolutionary Algorithm (EA). Such approaches promote the formation of multiple stable subpopulations within a population and empower the EA to locate multiple optimal or suboptimal solutions in parallel.[21,22] The success of EAs in real-world applications has also been verified by their uses of niching methods. For instance, a new mulching method was used to solve two optimization applications such as varied-line-spacing holographic grating design problem and the protein structure prediction problem on a lattice model.[23] The obtained results and the statistical analyses show the effectiveness of multimodal approaches compared with other single-modal methods. Three real world application examples were solved using a PSO-based MO method, called CLPSO, and the results indicated the ability of MO methods to locate the global optimum solutions for the problems.[24] EAs have also been applied in mechanics as well.[25]

Many niching methods have been proposed in the EA literature. Among all, the method proposed by Li[21] is a fast, powerful and effective approach for solving multimodal optimization problems. It involves a niching method incorporated in to PSO algorithm to form several implicit subpopulations within the main population, without the need to fix several additional niche parameters. Moreover, a memory mechanism is adopted to maintain found solutions during the search process.

In this paper, r2PSO algorithm, which is one of the PSO-based algorithms introduced by Li, is applied to estimate the location and size of an open edge crack in FGM cantilever beam. No previous works have been done regarding the crack identification by this method in FGM beams. The governing equation and boundary conditions are obtained by using the extended Hamilton's principle. By employing the boundary conditions, the characteristic equation is obtained as a function of position ratio of crack, depth ratio of crack, and the Young modulus ratio. Three natural frequencies of beam are evaluated from an analytic solution for a considered Young modulus, once the location and depth of crack are determined. Inversely, the first three natural frequencies are considered as inputs to the r2PSO algorithm. The algorithm evaluated the location and size of crack by minimizing the sum of the absolute value of characteristic equation for three natural frequencies.

2. THE ROTATIONAL SPRING FGM BEAM MODEL

The problem considered here a cantilever FGM beam of length L and thickness h, containing an edge crack of depth a located at position L_1 from the clamped end is shown schematically in Fig. 1. Young modulus and density of beam vary in the thickness direction according to exponential form as

$$E(z) = E_1\sqrt{k}e^{[(z/h)Ln(k)]};$$
$$\rho(z) = \rho_1\sqrt{k}e^{[(z/h)Ln(k)]}; \quad \nu = \nu_1; \tag{2}$$

where E_1, ρ_1, ν_1 are Young's modulus, density, and Poisson's ratio at $z = -h/2$, respectively, and E_2 is the Young's modulus at $z = h/2$. Moreover, k dictates the material variation profile through the thickness of the beam and equals $k = E_2/E_1$. For three values k 0.2, 1, and 5, the material distribution in the thickness direction of the Exponentially Functionally Graded Material beams is depicted in Fig. 1. As shown in Fig. 1, for $k = 1$, the material properties are homogenous and isotropy.

Figure 2 shows the layout of an FGM cantilevered beam and an edge crack is located at a distance of L_1 from the clamped end. The assumptions considered in this problem are that the crack is perpendicular to the beam surface and always remains open; the crack section is modeled as an elastic rotational spring which has no mass and no length; the in-plane inertia and rotary inertial effects of the beam are negligible; and the entire beam is divided into two sub-beams, connected by the rotational spring whose bending stiffness of the cracked section is related to the compliance G by

$$k_T = \frac{1}{G}; \tag{2a}$$

where the expression of G is derived on the basis of Erdogan and Wu's study,[26,27] in terms of the crack depth ratio as

$$G = \int_0^{\zeta} \frac{72\pi(1-\nu^2)\zeta F^2(\zeta)}{E(\zeta h)h^2}d\zeta; \quad \zeta = \frac{a}{h}; \quad \zeta \leq 0.7; \tag{2b}$$

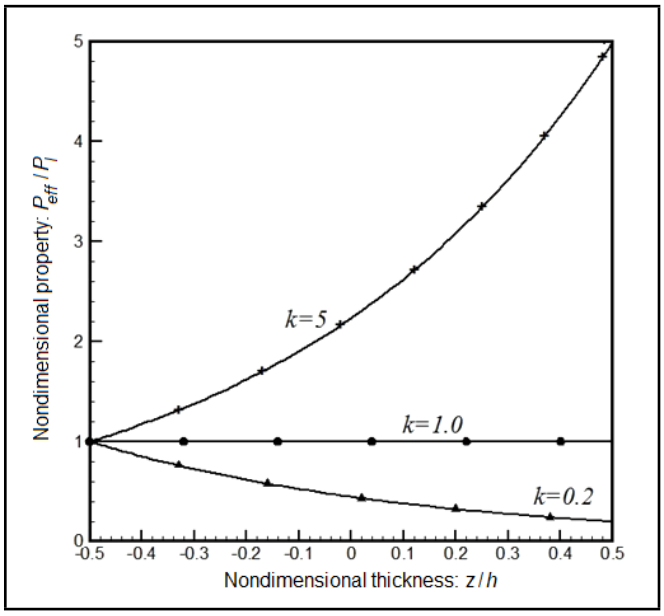

Figure 1. The variation of material properties in an E-FGM beam.

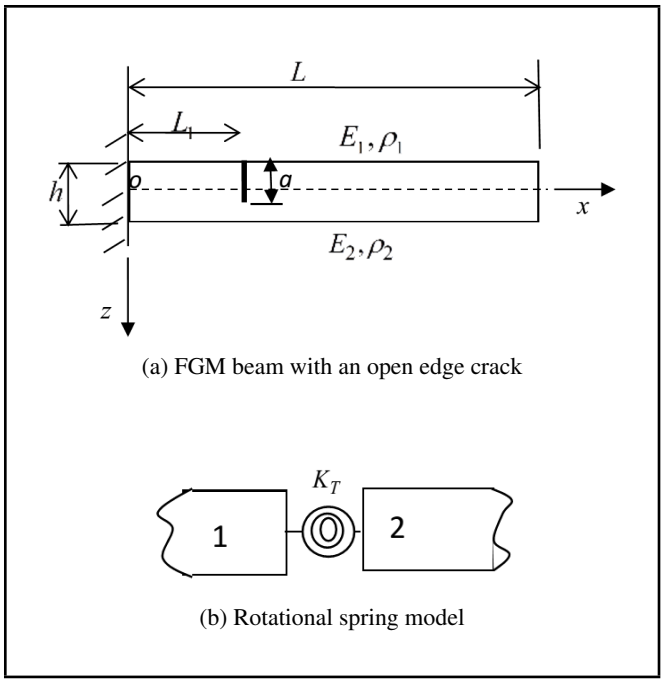

(a) FGM beam with an open edge crack

(b) Rotational spring model

Figure 2. Schematic of cantilever beam and crack model.

in which

$$F(\zeta) = 395.919\zeta^7 - 971.767\zeta^6 + 1009.567\zeta^5 - 554.549\zeta^4 + 170.387\zeta^3 - 24.225\zeta^2 + 0.300\zeta + 1.762; \quad \text{for} \quad \frac{E_2}{E_1} = 0.2; \tag{2c}$$

$$F(\zeta) = -1031.750\zeta^7 + 2395.830\zeta^6 - 2124.310\zeta^5 + 909.375\zeta^4 - 192.451\zeta^3 + 21.667\zeta^2 - 1.662\zeta + 1.150; \quad \text{for} \quad \frac{E_2}{E_1} = 1; \tag{2d}$$

$$F(\zeta) = -122.978\zeta^7 + 296.701\zeta^6 - 249.533\zeta^5 + 94.003\zeta^4 - 12.567\zeta^3 + 0.860\zeta^2 + 0.300\zeta + 0.605; \quad \text{for} \quad \frac{E_2}{E_1} = 5; \tag{2e}$$

The bending stiffness of the cross section can be determined from Eqs. (2a) and (2b).

3. GOVERNING EQUATIONS

Based on Euler-Bernoulli beam theory, the axial displacement, $u(x, y, z, t)$, and the transverse displacement of any point of the beam, $w(x, y, z, t)$, are given as

$$u(x, y, z, t) = u_0(x, t) - z\frac{\partial w_0(x, t)}{\partial x};$$
$$w(x, y, z, t) = w_0(x, t); \tag{3}$$

where $u_0(x, t)$, $w_0(x, t)$ are displacement components on the neutral axis. The strain-displacement and stress-strain relations could be given as

$$\varepsilon_{xx} = \varepsilon^0_{xx} + z\varepsilon^1_{xx}; \quad \varepsilon^0_{xx} = \frac{\partial u_0}{\partial x}; \quad \varepsilon^1_{xx} = -\frac{\partial^2 w_0}{\partial x^2}; \tag{3a}$$

$$\begin{bmatrix}\sigma_{xx}\\ \sigma_{yy}\\ \sigma_{zz}\end{bmatrix} = \begin{bmatrix}Q_{11} & Q_{12} & 0\\ Q_{21} & Q_{22} & 0\\ 0 & 0 & Q_{66}\end{bmatrix}\begin{bmatrix}\varepsilon_{xx}\\ \varepsilon_{yy}\\ \gamma_{xy}\end{bmatrix}; \tag{3b}$$

$$Q_{11} = Q_{22} = \frac{E}{1-\nu^2}; \quad Q_{12} = Q_{21} = \frac{E\nu}{1-\nu^2};$$
$$Q_{66} = \frac{E}{2(1+\nu)}; \tag{3c}$$

where ε^0_{xx}, ε^1_{xx} are strains due to mid-plane and bending, respectively.

For the cracked FGM beam, variation of kinetic energy and potential energy are of the form

$$\delta T = -\int_0^{L_1}\int_{-h/2}^{h/2} \rho(\ddot{u}\delta u + \ddot{w}\delta w)b\,dz\,dx \; - \int_{L_1}^{L}\int_{-h/2}^{h/2} \rho(\ddot{u}\delta u + \ddot{w}\delta w)b\,dz\,dx; \tag{3d}$$

$$\delta V = \int_0^{L_1}\int_{-h/2}^{h/2} (\sigma_{xx}\delta\varepsilon_{xx})b\,dz\,dx + \int_{L_1}^{L}\int_{-h/2}^{h/2} (\sigma_{xx}\delta\varepsilon_{xx})b\,dz\,dx + K_T\left(\frac{\partial w_0(L_1^+)}{\partial x} - \frac{\partial w_0(L_1^-)}{\partial x}\right)\left(\frac{\partial \delta w_0(L_1^+)}{\partial x} - \frac{\partial \delta w_0(L_1^-)}{\partial x}\right). \tag{3e}$$

Substituting Eqs. (3d) and (3e) in to the extended Hamilton's principle given in Eq. (3f), and noting the fact that δu_0, δw_0 are arbitrary, the governing equation of motion for i^{th} segment $(i = 1, 2)$ are obtained in Eqs. (3g) and (3h)

$$\int_{t_1}^{t_2}(\delta T - \delta V) = 0; \quad \delta u_0 = \delta w_0 = 0; \quad \text{at} \quad t = t_1,\ t = t_2; \tag{3f}$$

$$\delta u_{oi}: \quad A_{11}\frac{\partial^2 u_{oi}}{\partial x^2} - B_{11}\frac{\partial^3 w_{oi}}{\partial x^3} = 0; \tag{3g}$$

$$\delta w_{oi}: \quad \left(D_{11} - \frac{B_{11}^2}{A_{11}}\right)\frac{\partial^4 w_{oi}}{\partial x^4} + I_1\ddot{w}_{oi} = 0; \tag{3h}$$

where subscript $i = 1, 2$ refer to the left sub-beam and right sub-beam, respectively, which is divided by the crack. The parameters I_1, A_{11}, B_{11}, D_{11} are defined as

$$I_1 = \int_{-h/2}^{h/2} \rho(z)dz; \quad (A_{11}, B_{11}, D_{11}) = \int_{-h/2}^{h/2} E(z)(1, z, z^2)dz. \tag{3i}$$

The boundary conditions are

$$u_0 = 0, \quad w_0 = 0, \quad \frac{\partial w_0}{\partial x} = 0 \quad \text{at} \quad x = 0; \tag{3j}$$

$$N_{xx} = 0, \quad M_{xx} = 0, \quad \frac{\partial M_{xx}}{\partial x} = 0 \quad \text{at} \quad x = L; \tag{3k}$$

$$u_{01} = u_{02}, \quad w_{01} = w_{02}, \quad N_{xx1} = N_{xx2}, \quad M_{xx1} = M_{xx2}, \quad \frac{\partial M_{xx1}}{\partial x} = \frac{\partial M_{xx2}}{\partial x}, \quad K_T \frac{dw_{01}}{dx} - M_{xx1} = K_T \frac{dw_{02}}{dx} \quad \text{at} \quad x = L_1; \tag{3l}$$

where the stress resultant N_{xx} (force per unit length) and the stress moment M_{xx} (moment per unit length), are defined as the following integral expressions:

$$N_{xx} = \int_{-h/2}^{h/2} \sigma_{xx}dz; \quad M_{xx} = \int_{-h/2}^{h/2} z\sigma_{xx}dz. \tag{3m}$$

4. FORWARD PROBLEM

In direct problems, the eigen solutions for the cantilevered boundary conditions are derived using the following separable solutions:

$$u_{oi}(x,t) = U_{oi}(x)e^{j\omega t}; \quad w_{oi}(x,t) = W_{oi}(x)e^{j\omega t}; \quad i = 1; \tag{4}$$

where ω is the natural frequency of the cracked FGM beam. Substituting Eq. (4) into Eqs. (3g) and (3h), the displacement solutions for two sub-beams are

$$W_{oi} = e_{i1}\sin(\lambda x) + e_{i2}\cos(\lambda x) + e_{i3}\sinh(\lambda x) + e_{i4}\cosh(\lambda x); \quad i = 1, 2; \tag{4a}$$

$$U_{oi} = \lambda(B_{11}/A_{11})\big[e_{i1}\cos(\lambda x) - e_{i2}\sin(\lambda x) + e_{i3}\cosh(\lambda x) - e_{i4}\sinh(\lambda x)\big] + g_i x + g_{i0}; \quad i = 1, 2; \tag{4b}$$

in which $\lambda = \sqrt[4]{(I_1\omega^2/d)}$, $d = \big(D_{11} - (B_{11}^2/A_{11})\big)$, the unknown e_{i1}, e_{i2}, e_{i3}, e_{i4} are to be determined from the compatibility conditions at the intersections of sub-beams and boundary conditions. Substituting Eqs. (4a) and (4b) into Eqs. (3j)–(3l) yields a matrix equation as

$$[H]\{q\} = 0; \tag{4c}$$

where H is a square matrix nonlinearly dependent on the natural frequency ω, q is a vector composed of 12 unknown parameters. The matrix H and the vector q are defined as Eq. (4d) (written on the next page), where

$$J_{10} = \sin(\lambda L); \quad J_{20} = \cos(\lambda L); \quad J_{30} = \sinh(\lambda L); \quad J_{40} = \cosh(\lambda L); \quad J_{11} = \sin(\lambda L_1); \quad J_{21} = \cos(\lambda L_1); \quad J_{31} = \sinh(\lambda L_1); \quad J_{41} = \cosh(\lambda L_1);$$

$$\{q\} = \big\{e_{11}\ e_{12}\ e_{13}\ e_{14}\ g_1\ g_{10}\ e_{21}\ e_{22}\ e_{23}\ e_{24}\ g_2\ g_{20}\big\}; \tag{4e}$$

thus, the characteristic equation which ensures the non-trivial solution is

$$\det\big([H(\lambda)]\big) = |H(\lambda)| = 0. \tag{4f}$$

This equation can be solved analytically for certain values of location and depth of crack and natural frequencies are obtained in this solution. The beam is examined for various crack depths at different locations to generate the test point. Each test point represents the measured frequency, which are used to evaluate the inverse algorithm to detect the depth and location of crack. The first three natural frequencies are inputs of the inverse algorithm.

5. INVERSE PROBLEM

For the inverse problem of the cracked system, the measured frequencies based on the calculations of forward problem are entered as input. These values are used instead of experimental measurements. Several non-linear equation solving algorithms can be used for this problem. In this paper, these unknown parameters are solved by using the r2PSO algorithm.[21]

In crack detection process, the first three natural frequencies are measured analytically from the characteristic equation by considering the values for location and depth of crack which is named as reference location and depth. Then for simulation of experimental data, the error percentage is added to these measured values, and are then entered as input to the inverse algorithm. The ratio of natural frequency $(\omega_{ci}/\omega_{oi})^*$ as input of the inverse algorithm is expressed in Eq. (5) as,

$$(\omega_{ci}/\omega_{oi})^* = (\omega_{ci}/\omega_{oi})^c + err \times \varepsilon_i; \quad i = 1, 2, 3; \tag{5}$$

where ε is a random number at interval $[-0.5, 0.5]$, err is the rate magnitude of error $(0\%, 1\%, 2\%)$ and $(\omega_{ci}/\omega_{oi})^c$ is the rate of measured natural frequency. The r2PSO algorithm evaluated the location and depth of crack for different value of $(\omega_{ci}/\omega_{oi})^*$. The obtained values of location and depth are compared to the values of references. The objective function based on characteristic equation is defined as

$$f = |H(\lambda)|_{\lambda=\lambda_1} + |H(\lambda)|_{\lambda=\lambda_2} + |H(\lambda)|_{\lambda=\lambda_3}; \tag{5a}$$

where $\lambda_i (i = 1, 2, 3) = \sqrt[4]{(I_1\omega_{ci}^2/d)}$, and ω_{ci} is obtained from the natural frequency ratio $(\omega_{ci}/\omega_{oi})^*$ expressed in Eq. (5).

5.1. Crack Detection in FGM Beam Using R2PSO

In Li's method, an *lbest* PSO using a ring topology was used to induce stable niching behaviours. For each particle, a neighborhood is considered to contain two or three members of the population with their personal bests (memories), in

$$[H]=\begin{bmatrix}
0 & 0 & 0 & 0 & 0 & 1 & 0 & 0 & 0 & 0 & 0 & 0\\
0 & 1 & 0 & 1 & 0 & 0 & 0 & 0 & 0 & 0 & 0 & 0\\
1 & 0 & 1 & 0 & 0 & 0 & 0 & 0 & 0 & 0 & 0 & 0\\
0 & 0 & 0 & 0 & 0 & 0 & 0 & 0 & 0 & 0 & 1 & 0\\
0 & 0 & 0 & 0 & 0 & 0 & J_{10} & J_{20} & -J_{30} & -J_{40} & \frac{B_{11}}{d\lambda^2} & 0\\
0 & 0 & 0 & 0 & 0 & 0 & -J_{20} & J_{10} & J_{40} & J_{30} & 0 & 0\\
\frac{\lambda B_{11}}{A_{11}}J_{21} & -\frac{\lambda B_{11}}{A_{11}}J_{11} & \frac{\lambda B_{11}}{A_{11}}J_{41} & \frac{\lambda B_{11}}{A_{11}}J_{31} & L_1 & 1 & -\frac{\lambda B_{11}}{A_{11}}J_{21} & \frac{\lambda B_{11}}{A_{11}}J_{11} & -\frac{\lambda B_{11}}{A_{11}}J_{41} & -\frac{\lambda B_{11}}{A_{11}}J_{31} & -L_1 & -1\\
J_{11} & J_{21} & J_{31} & J_{41} & 0 & 0 & -J_{11} & -J_{21} & -J_{31} & -J_{41} & 0 & 0\\
0 & 0 & 0 & 0 & 1 & 0 & 0 & 0 & 0 & 0 & -1 & 0\\
-J_{11} & -J_{21} & J_{31} & J_{41} & \frac{B_{11}}{d\lambda^2} & 0 & J_{11} & J_{21} & -J_{31} & -J_{41} & \frac{B_{11}}{d\lambda^2} & 0\\
-J_{21} & J_{11} & J_{41} & J_{31} & 0 & 0 & J_{21} & -J_{11} & -J_{41} & -J_{31} & 0 & 0\\
J_{21}-\frac{\lambda d}{K_T}J_{11} & -J_{11}-\frac{\lambda d}{K_T}J_{21} & J_{41}+\frac{\lambda d}{K_T}J_{31} & J_{31}+\frac{\lambda d}{K_T}J_{41} & \frac{-B_{11}}{K_T\lambda} & 0 & -J_{21} & J_{11} & -J_{41} & -J_{31} & 0 & 0
\end{bmatrix}; \tag{4d}$$

which the best member acts as the best neighborhood in order to update velocity and position of corresponding neighborhood members. The velocity and position of i^{th} particle is updated according to Eqs. (5b) and (5c)

$$\vec{v}_i = \xi\big(\vec{v}_i + \vec{R}_1[0,\varphi_1]\otimes(\vec{P}_i-\vec{x}_i) + \vec{R}_2[0,\varphi_2]\otimes(\vec{P}_{n,i}-\vec{x}_i)\big); \tag{5b}$$

$$\vec{x}_i \leftarrow \vec{x}_i + \vec{v}_i; \tag{5c}$$

where $\vec{P}_{n,i}$ denotes the neighborhood best (or a local leader) of i^{th} particle found in its corresponding neighborhood. $\vec{R}_1[0,\varphi_1]$ and $\vec{R}_2[0,\varphi_2]$ are two separate functions each returning a vector comprising random values uniformly generated in the ranges $[0,\varphi_1]$ and $[0,\varphi_2]$, respectively. χ is a constant and φ_1 and φ_2 are commonly set to $\varphi/2$ (where φ is a positive constant). The symbol $\otimes$ denotes point-wise vector multiplication.

Depending on how the neighborhoods are formed and interacted in *lbest* PSO, four variants of this method are presented:[21] (1,2) r2PSO and r3PSO, in which each neighborhood contains 2 or 3 particles of contiguous indices in PSO population respectively, and after formation of such neighborhoods, they are considered to be overlapped. It means that different neighborhoods can share some members; (3,4) r2PSO-lhc and r3PSO-lhc, where the neighborhoods are formed with 2 or 3 members, respectively without overlap between neighborhoods. In these variants each neighborhood acts like a local hill climber to explore the search space and no information is exchanged between different neighborhoods. The number of members of each neighborhood and overlap between them controls the tendency of algorithm to find global or local optima. More members and overlapping neighborhoods lead the algorithm to tend toward locating more dominant peaks over other less dominant peaks. If the goal of optimization is to locate both global and local peaks, removing the overlapping neighborhoods in the ring topology can cause finding local optima as well as global optima of the search space.

In this paper, the goal is to find a global optimum solution for the problem. Therefore, the overlapped variants of local best variants seem more appropriate. Thus, we used the r2PSO variant using the following settings: number of iterations = 100, population size = 100, max velocity = 0.4, min velocity = -0.4, and . Table 1 shows the pseudo code of *lbest* PSO.

Table 1. The pseudo code of *lbest* PSO using a ring topology (with three neighbors).[21]

```
Randomly generate an initial population
repeat
  for i = 1 to Population Size do
    if fit(x_i) > fit(p_i) then p_i ← x_i
  end
  for i = 1 to Population Size do
    p_{n,i} ← neighborhoodBest(p_{i-1}, p_i, p_{i+1});
  end
  for i = 1 to Population Size do
    Equation (4f);
    Equation (5);
  end
until termination criterion is met;
```

Table 2. Fundamental frequency ratio ω_1/ω_{01} of an isotropic homogenous cantilevered beam ($L/h = 4.0$, $\nu = 0.3$, $a/h = 0.2$).

$L_1/L = 0.2$		$L_1/L = 0.4$		$L_1/L = 0.6$	
Ref.[28]	This paper (analytical solution)	Ref.[28]	This paper (analytical solution)	Ref.[28]	This paper (analytical solution)
0.94101	0.96556	0.96667	0.98563	0.99583	0.99637

6. NUMERICAL RESULTS

6.1. Forward Solution Verification

In order to validate the accuracy of analytical solution of direct problem, the fundamental frequency ratio ω_1/ω_{10} of a

Table 3. First three dimensionless natural frequencies of intact FGM cantilevered beams ($E_1 = 70$ GPa, $\nu = 0.33$, $\rho = 2780$ kg/m^3).

		$\overline{\omega}_1$		$\overline{\omega}_2$		$\overline{\omega}_3$	
L/h	E_2/E_1	Ref.[8]	Analytical solution	Ref.[8]	Analytical solution	Ref.[8]	Analytical solution
20	0.2	0.83	0.83	5.18	5.18	14.49	14.49
	1	0.88	0.88	5.51	5.51	15.42	15.42
	5	0.83	0.83	5.18	5.18	14.49	14.49
10	0.2	3.30	3.30	20.70	20.70	57.97	57.97
	1	3.52	3.52	22.03	22.03	61.70	61.70
	5	3.30	3.30	20.70	20.70	57.97	57.97

Table 4. Comparison of reference crack parameters with the predicted values obtained by inverse algorithm ($E_2/E_1 = 0.2$) and r2PSO (average of best solutions found in ten independent runs).

Reference crack			Predicted crack by r2PSO			
a/h	L_1/L	err (%)	a/h	Rate of error	L_1/L	Rate of error
0.3	0.2	0	0.3025	0.86	0.2008	0.41
		1	0.2971	0.93	0.2019	0.99
		2	0.2958	1.38	0.2031	1.58
	0.4	0	0.3009	0.32	0.4027	0.68
		1	0.3021	0.71	0.4030	0.76
		2	0.3025	0.84	0.4032	0.82
0.5	0.2	0	0.5011	0.23	0.1991	0.41
		1	0.4956	0.87	0.2140	0.72
		2	0.4954	0.91	0.2023	1.16
	0.4	0	0.5028	0.56	0.4007	0.19
		1	0.4968	0.62	0.4022	0.56
		2	0.5034	0.69	0.4039	0.98
0.7	0.2	0	0.6981	0.25	0.2010	0.53
		1	0.7051	0.74	0.2011	0.55
		2	0.6936	0.90	0.2020	1.01
	0.4	0	0.6948	0.74	0.4039	0.90
		1	0.6942	0.82	0.4051	1.27
		2	0.6934	0.93	0.4067	1.67

cracked cantilevered isotropic beam is computed at different locations. Moreover, ω_{10} is the first natural frequency of the intact beam. Table 2 shows the fundamental frequency ratio of an isotropic homogenous cantilevered beam with the properties $L/h = 4.0$, $\nu = 0.3$, $a/h = 0.2$. This example was previously analyzed by Yokoyama and Chen[28] using the finite element method and Bernoulli–Euler beam theory. As shown in Table 2, our analytical solutions are compatible with the finite element results.

In Table 3, the lowest three modal frequencies of the intact FGM cantilevered beam are calculated by the r2PSO method and compared with those reported by Yu and Chu.[8] In the Yu and Chu's work the p-FEM was used for the calculation of frequencies and the modal frequencies were normalized as $\overline{\omega}_n = \omega_n/(\sqrt{d_0/I_0})$, where d_0 and I_0 are the corresponding values of d_0 and I_0 of an isotropic homogeneous beam $E_2/E_1 = 1$. Table 3 shows that the obtained results are in conformity with the results of the paper.[8]

6.2. Crack Identification by R2PSO Algorithm

The cracked cantilever FGM beam is made of a material with properties $E_1 = 70$ GPa, $\nu = 0.33$, $\rho = 2780$ kg/m^3 and with geometric data $L = 2$ m, $h = 0.1$ m.

The location and depth of crack is calculated by r2PSO algorithm for three cases $E_2/E_1 = 0.2$, $E_2/E_1 = 1$, $E_2/E_1 = 5$ as shown in Tables 4–6, respectively.

In crack detection process for three cases, by selecting the reference location and depth of crack, the first three natural frequencies are obtained from the direct solution and subsequently the ratio of measured natural frequencies $(\omega_{ci}/\omega_{oi})^*$ is computed. Then, by estimating random number (ε) for 10 times in Eq. (5), the 10 ratio of natural frequencies $(\omega_{ci}/\omega_{oi})^*$ are entered as inputs to the r2PSO algorithm. The algorithm was run 10 times to compute the location and depth of crack.

Table 5. Comparison of reference crack parameters with the predicted values obtained by inverse algorithm ($E_2/E_1 = 1$) and r2PSO (average of best solutions found in ten independent runs).

Reference crack			Predicted crack by r2PSO			
a/h	L_1/L	err (%)	a/h	Rate of error	L_1/L	Rate of error
0.3	0.2	0	0.2997	0.073	0.2010	0.53
		1	0.3007	0.23	0.2015	0.78
		2	0.3035	1.19	0.1970	1.48
	0.4	0	0.3020	0.68	0.4033	0.83
		1	0.3033	1.13	0.4044	1.12
		2	0.2946	1.77	0.3946	1.33
0.5	0.2	0	0.4958	0.82	0.2014	0.71
		1	0.5046	0.92	0.2023	1.16
		2	0.4937	1.25	0.2027	1.36
	0.4	0	0.4978	0.43	0.3979	0.50
		1	0.5061	1.23	0.4035	0.88
		2	0.4909	1.80	0.4073	1.82
0.7	0.2	0	0.7015	0.21	0.1987	0.64
		1	0.6932	0.96	0.2014	0.72
		2	0.6884	1.65	0.2038	1.93
	0.4	0	0.6984	0.22	0.4031	0.78
		1	0.6948	0.77	0.4052	1.32
		2	0.6932	0.96	0.4054	1.36

Table 6. Comparison of reference crack parameters with the predicted values obtained by inverse algorithm ($E_2/E_1 = 5$) and r2PSO (average of best solutions found in ten independent runs).

Reference crack			Predicted crack by r2PSO			
a/h	L_1/L	err (%)	a/h	Rate of error	L_1/L	Rate of error
0.3	0.2	0	0.2973	0.89	0.2010	0.52
		1	0.3031	1.03	0.2018	0.93
		2	0.2963	1.22	0.2019	0.96
	0.4	0	0.3006	0.23	0.4024	0.61
		1	0.2923	0.25	0.4025	0.64
		2	0.2991	0.27	0.4050	1.25
0.5	0.2	0	0.5028	0.56	0.1990	0.47
		1	0.5039	0.79	0.2012	0.60
		2	0.5042	0.84	0.2022	1.10
	0.4	0	0.4990	0.19	0.3989	0.25
		1	0.5054	1.08	0.4027	0.68
		2	0.4940	1.18	0.4035	0.89
0.7	0.2	0	0.6975	0.35	0.2001	0.05
		1	0.7038	0.54	0.2004	0.22
		2	0.6949	0.72	0.1992	0.37
	0.4	0	0.7007	0.10	0.4028	0.72
		1	0.6945	0.78	0.4036	0.90
		2	0.6936	0.90	0.4046	1.15

By averaging the 10 obtained best values, the predicted location and depth values of crack are acquired.

Tables 4–6 present the comparisons between reference crack parameters with obtained crack parameters for different error measurements in various scenarios. As shown in Tables 4–6, when the measurement and modeling error are increased, the precision of position and depth of crack is decreased.

In order to illustrate the performance of r2PSO algorithm compared to the other algorithms in terms of the convergence speed, the averaged best so far diagrams of three algorithms, namely PSO, GA, and r2PSO. These three are depicted over 10 independent runs in Fig. 3 and provided that $E_1/E_2 = 0.2$, $a/h = 0.7$, $L_1/L = 0.2$, $err = 0\%$. Similar diagrams for two other scenarios: $E_1/E_2 = 1$, $a/h = 0.7$, $L_1/L = 0.2$, $err = 0\%$, and for $E_1/E_2 = 5$, $a/h = 0.7$, $L_1/L = 0.2$, $err = 0\%$ are shown in Figs. 4 and 5.

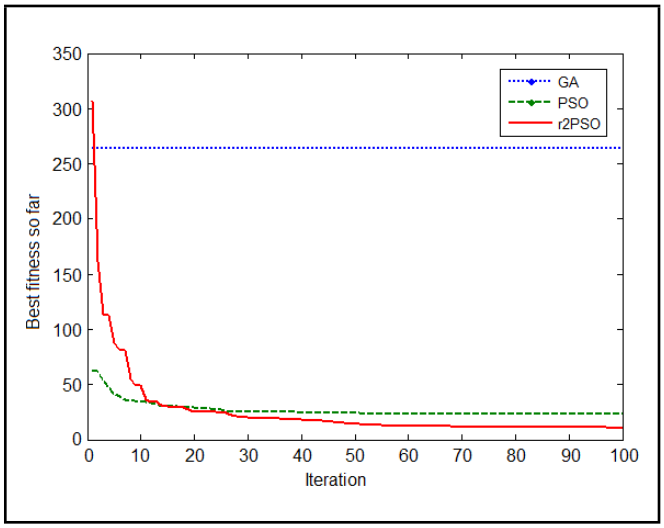

Figure 3. Convergence diagram for $E_1/E_2 = 0.2$, $a/h = 0.7$, $L_1/L = 0.2$, $err = 0\%$.

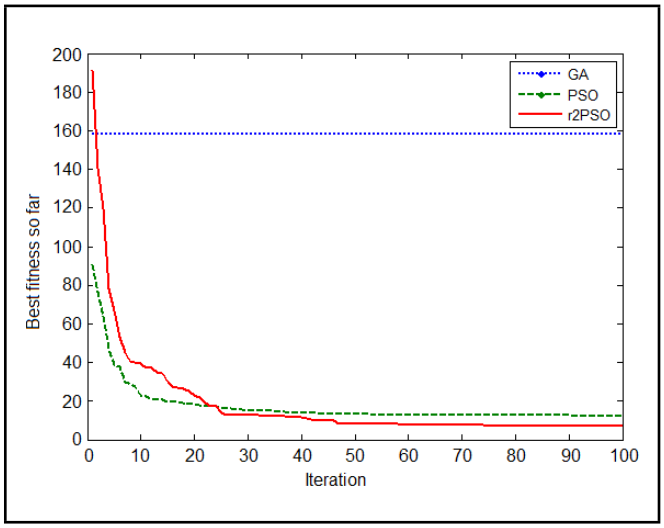

Figure 4. Convergence diagram for $E_1/E_2 = 1$, $a/h = 0.7$, $L_1/L = 0.2$, $err = 0\%$.

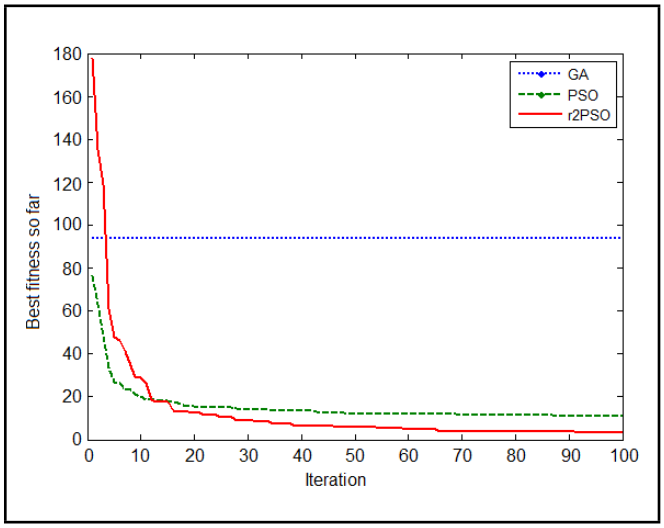

Figure 5. Convergence diagram for $E_1/E_2 = 5$, $a/h = 0.7$, $L_1/L = 0.2$, $err = 0\%$.

7. CONCLUSIONS

The r2PSO algorithm has been implemented in this article to detect the crack in a cantilever FGM beam. The Euler-Bernoulli beam theory was considered for modeling the beam and the open edge crack was replaced by a linear rotational spring. The natural frequencies of FGM beam were obtained from analytical solution. Knowing the natural frequencies, the crack location and depth are calculated in inverse problem. The inverse problem was defined as an optimization problem. The objective function was based on the absolute value of characteristic equation. Summation of first, second and third characteristic equation corresponding to first, second and third natural frequencies was the cost function. Then this cost function was considered as the fitness function in r2PSO algorithm. Comparing the results obtained by r2PSO with those achieved by GA and PSO reveals the applicability and efficiency of r2PSO in finding optimal solutions within a reasonable time.

REFERENCES

[1] Lee, J. Identification of multiple cracks using natural frequencies, *Journal of Sound and Vibration*, **320** (3), 482–490, (2009). https://dx.doi.org/10.1016/j.jsv.2008.10.033

[2] Sekhar, A. S. Crack identification in a rotor system: a model-based approach, *Journal of Sound and Vibration*, **270**, 887–902, (2004). https://dx.doi.org/10.1016/s0022-460x(03)00637-0

[3] Kitipornchai, S., Yang, J., and Liew, K. M. Semi-analytical solution for nonlinear vibration of laminated FGM plates with geometric imperfections, *International Journal of Solids and Structures*, **41**, 2235–2257, (2004). https://dx.doi.org/10.1016/j.ijsolstr.2003.12.019

[4] Allahverdizadeh, A., Naei, M. H., and Nikkhah Bahrami, M. Nonlinear free and forced vibration analysis of thin circular functionally graded plates, *Journal of Sound and Vibration*, **310**, 966–984, (2008). https://dx.doi.org/10.1016/j.jsv.2007.08.011

[5] Woo, J., Meguid, S. A., and Ong, L. S. Nonlinear free vibration behavior of functionally graded plates, *Journal of Sound and Vibration*, **289**, 595–611, (2006). https://dx.doi.org/10.1016/j.jsv.2005.02.031

[6] Matsunaga, H. Free vibration and stability of functionally graded shallow shells according to a 2-D higher-order deformation theory, *Composite Structures*, **84**, 132–146, (2008). https://dx.doi.org/10.1016/j.compstruct.2007.07.006

[7] Aydogdu, M. and Taskin, V. Free vibration analysis of functionally graded beams with simply supported edges, *Materials & Design*, **28**, 1651–1656, (2007). https://dx.doi.org/10.1016/j.matdes.2006.02.007

[8] Yu, Z. and Chu, F. Identification of crack in functionally graded material beams using the p-version of finite element method, *Journal of Sound and Vibration*, **325**, 69–84, (2009). https://dx.doi.org/10.1016/j.jsv.2009.03.010

[9] Wei, D., Liu, Y., and Xiang, Z. An analytical method for free vibration analysis of functionally graded beams with edge cracks, *Journal of Sound and Vibration*, **331** (7), 1686–1700, (2012). https://dx.doi.org/10.1016/j.jsv.2011.11.020

[10] Xiang, J., Zhong, Y., Chen, X., and He, Z., Crack detection in a shaft by combination of wavelet-based elements, *International Journal of Solids and Structures*, **45**, 4782–4795, (2008). https://dx.doi.org/10.1016/j.ijsolstr.2008.04.014

[11] Vakil Baghmishe, M. T., Peimani, M., Sadeghi, M. H., and Ettefagh, M. Crack detection in beam-like structures using genetic algorithms, *Applied Soft Computing*, **8**, 1150–1160, (2008). https://dx.doi.org/10.1016/j.asoc.2007.10.003

[12] Kang, F., Li, J., and Xu, Q. Damage detection based on improved particle swarm optimization using vibration data, *Applied Soft Computing*, **12**, 2329–2335, (2012). https://dx.doi.org/10.1016/j.asoc.2012.03.050

[13] Kitipornchai, S., Ke, L. L., Yang, J., and Xiang, Y. Nonlinear vibration of edge cracked functionally graded Timoshenko beams, *Journal of Sound and Vibration*, **324**, 962–982, (2009). https://dx.doi.org/10.1016/j.jsv.2009.02.023

[14] Fernando, S., Buezas, B., Marta, R. C., and Filipich, P. Damage detection with genetic algorithms taking in to account a crack contact model, *Engineering Fracture Mechanics*, **78** (4), 695-712, (2011). https://dx.doi.org/10.1016/j.engfracmech.2010.11.008

[15] Birman, V. and Byrd, L. W. Vibration of damaged cantilevered beams manufactured from functionally graded materials, *AIAA Journal*, **45**, 2747–2757, (2007). https://dx.doi.org/10.2514/1.30076

[16] Aydin, K. Free vibration of functionally graded beams with arbitrary number of surface cracks, *European Journal of Mechanics—A/Solids*, **42**, 112–124, (2013). https://dx.doi.org/10.1016/j.euromechsol.2013.05.002

[17] Miguel, L. F. F., Lopez, R. H., and Miguel, L. F. F. A hybrid approach for damage detection of structures under operational conditions, *Journal of Sound and Vibration*, **332**, 4241–4260, (2013). https://dx.doi.org/10.1016/j.jsv.2013.03.017

[18] Vakil Baghmishe, M. T., Peimani, M., Sadeghi, M. H., Ettefagh, M., and Tabrizi, A. F. A hybrid particle swarm Nelder-Mead optimization method for crack detection in cantilever beams, *Applied Soft Computing*, **12**, 2217–2226, (2012). https://dx.doi.org/10.1016/j.asoc.2012.03.030

[19] Sahoo, B. and Maity, D. Damage assessment of structures using hybrid neuro-genetic algorithm, *Applied Soft Computing*, **7**, 89–104, (2007). https://dx.doi.org/10.1016/j.asoc.2005.04.001

[20] Moradi, S., Razi, P., and Fatahi, L. On the application of bees algorithm to the problem of crack detection of beam-type structures, *Computers and Structures*, **89**, 2169–2175, (2011). https://dx.doi.org/10.1016/j.compstruc.2011.08.020

[21] Li, X. Niching without niching parameters: particle swarm optimization using a ring topology, *IEEE Transactions on Evolutionary Computation*, **14**, 150–169, (2010). https://dx.doi.org/10.1109/tevc.2009.2026270

[22] Roy, S., Islam, Sk. M., Das, S., and Ghosh, S. Multimodal optimization by artificial weed colonies enhanced with localized group search optimizers, *Applied Soft Computing*, **13**, 27–46, (2013). https://dx.doi.org/10.1016/j.asoc.2012.08.038

[23] Wong, K. C., Ricky, C. H. W., Mok, K. P., Chengbin P., and Zhaolei Z. Evolutionary multimodal optimization using the principle of locality, *Information Science*, **13**, 138–170, (2012). https://dx.doi.org/10.1016/j.ins.2011.12.016

[24] Lei, G. and Atakelty, H. Comprehensive learning particle swarm optimizer for constrained mixed-variable optimization problems, *International Journal of Computational Intelligence Systems*, **3** (6), 832–842, (2010). https://dx.doi.org/10.1080/18756891.2010.9727745

[25] Eftekhari, M., Mahzoon, M., and Ziaei Rad, S. An evolutionary search technique to determine natural frequencies and mode shapes of composite Timoshenko beams, *Mechanics Research Communications*, **38** (3), 220–225, (2011). https://dx.doi.org/10.1016/j.mechrescom.2011.02.012

[26] Broek, D. *Elementary Engineering Fracture Mechanics*, Martinus Nijhoff Publishers, Dordrecht, (1986). https://dx.doi.org/10.1007/978-94-009-4333-9

[27] Erdogan, F. and Wu, B. H. The surface crack problem for a plate with functionally graded properties, *Journal of Applied Mechanics*, **64**, 448–456, (1997). https://dx.doi.org/10.1115/1.2788914

[28] Yokoyama, T. and Chen, M. C. Vibration analysis of edge-cracked beams using a line-spring model, *Engineering Fracture Mechanics*, **59** (3), 403–9, (1998). https://dx.doi.org/10.1016/s0013-7944(97)80283-4